Journal of the Optical Society of America B
OPTICAL PHYSICS

Manipulating multi-frequency light in a five-level cascade-type atomic medium associated with giant self-Kerr nonlinearity

Anh Nguyen Tuan,[1,2] Doai Le Van,[1] and Bang Nguyen Huy[1,*]

[1]Vinh University, 182 Le Duan Street, Vinh City, Vietnam
[2]Ho Chi Minh City University of Food Industry, Ho Chi Minh City, Vietnam
*Corresponding author: bangnh@vinhuni.edu.vn

Received 8 January 2018; revised 18 March 2018; accepted 6 April 2018; posted 11 April 2018 (Doc. ID 319164); published 2 May 2018

We propose a model to manipulate group velocity of a multi-frequency probe light in an electromagnetically induced transparency medium consisting of five-level cascade-type atoms associated with a giant self-Kerr nonlinearity. An analytic expression of group index for the probe light is derived as a function of parameters of the probe and coupling fields, atomic density, and lifetimes of excited atomic states. In the presence of the self-Kerr, both probe and controlling fields can be used as knobs to manipulate the probe light between the subluminal and superluminal propagation modes in three separated frequency regions. The theoretical model agrees with experimental observation, and it is helpful to find the optimized parameters and related applications. Furthermore, by using such a cascade excitation scheme, it could be possible to choose the uppermost excited electronic states having long lifetimes, as Rydberg states, to slow the light down to a few mm/s.

OCIS codes: (020.1670) Coherent optical effects; (190.3270) Kerr effect; (350.5500) Propagation.

https://doi.org/10.1364/JOSAB.35.001233

1. INTRODUCTION

Controlling group velocity of light has been one of the most interesting topics in optical science during the last two decades due to its having potential important applications, such as controllable optical delay lines, optical switching, telecommunication, interferometry, optical data storage and optical memories, quantum information processing, and so on [1–4]. In general, slow light or subluminal propagation takes place in a normal dispersive medium, while fast light or superluminal propagation is associated with an anomalous dispersive medium.

The advent of electromagnetically induced transparency (EIT) delivers media of reduced resonant absorption and steep dispersion for a probe light [5]. Furthermore, magnitude and sign of dispersion of the medium can be controlled by a coupling light. Using the EIT technique, several researchers attempted to demonstrate experimentally the subluminal [6–10] and superluminal [11–14] propagation of light. Other studies concerned switching between the subluminal and superluminal light propagation in an atomic medium by changing frequency, intensity, phase, and polarization of applied fields [15–25].

In addition to steep dispersion, another interesting property of the EIT medium is exhibition of giant Kerr nonlinearity with controllable magnitude and sign [26,27]. As a consequence, such a giant Kerr nonlinearity influences the group velocity of light in the EIT media, even at very low light intensity. Indeed, Agarwal *et al.* [28] demonstrated that cross-Kerr nonlinearity makes a significant contribution to the group velocity. More recently, Ali *et al.* [29] showed that the light could be further slowed by the cross-Kerr nonlinearity. In addition to the cross-Kerr, a giant self-Kerr nonlinearity also arises in the EIT medium [5], but it is still not taken into account in slowing-light studies so far. In addition, a lack of precise description of the group velocity of light hampers applications concerning manipulation of light in EIT media.

In the early years of EIT study, most interest focused on the three-level systems to create a single EIT window in which the light can be controlled only in a narrow frequency region. From a practical perspective, extension from a single- to multi-window EIT is apparently of interest due to its promising applications in multichannel optical communication, waveguides for optical signal processing, and multichannel quantum information processing. A possible way to obtain a multi-EIT window is to use additionally controlling fields to excite various multi-level atomic systems [30,31]. Some researchers used such a technique to control the group velocity at multiple frequencies [19,23,31,32].

Another simpler way is to use only a controlling field to couple simultaneously several closely spaced hyperfine levels, which was first demonstrated in a five-level cascade system [33]. The first advantage of the five-level cascade scheme is that it is possible to simultaneously slow probe light at different frequencies by controlling a sole coupling light. As discussed in Ref. [34], such slowed light has an advantage in producing the quantum entanglement. The second advantage is that it is possible to choose the uppermost excited states as the Rydberg states having long lifetimes (see Ref. [23]), which increases significantly atomic coherence or slower group velocity of the light. The third advantage arises from the presence of self-Kerr, so one may control between sub- and superluminal propagation modes by probe and/or coupling fields. This system has been studied recently by using an analytic method [35,36] and extended later to several applications, e.g., enhancement of Kerr nonlinearity [37,38], optical bistability (OB) [39], generating optical nano-fibers for guiding entangled beams [40], and optical soliton formation of laser pulses [41]. The analytic model has been used recently to interpret the experimental observations with a good agreement [42]. Growing from this interest, in this work, we propose to use a five-level cascade atomic medium to control a multi-frequency probe light by a sole light in the presence of giant self-Kerr nonlinearity. A possible way to switch between the subluminal and superluminal propagation mode is discussed.

2. THEORETICAL MODEL

We consider a cold atomic medium consisting of five-level cascade-type systems, as shown in Fig. 1. A weak probe laser beam (with frequency ω_p) excites the transition $|1\rangle \leftrightarrow |2\rangle$, whereas an intense controlling laser beam (with frequency ω_c) couples simultaneously transitions between the state $|2\rangle$ and three closely spaced states $|3\rangle$, $|4\rangle$, and $|5\rangle$. We denote δ_1 and δ_2 as frequency separations between the levels $|3\rangle - |4\rangle$ and $|5\rangle - |3\rangle$, respectively.

The frequency detuning of the probe and controlling lasers are, respectively, defined as

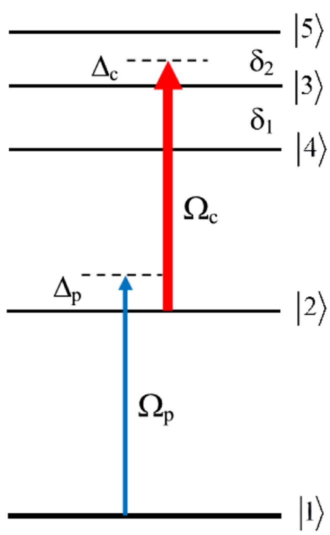

Fig. 1. Five-level cascade excitation scheme.

$$\Delta_p = \omega_p - \omega_{21}, \qquad \Delta_c = \omega_c - \omega_{32}. \tag{1}$$

In the framework of semiclassical theory, using the dipole and rotating wave approximations, the evolution of the system can be represented by the following density-matrix equations [35]:

$$\dot{\rho}_{55} = -\Gamma_{52}\rho_{55} - \frac{i}{2}\Omega_c a_{52}(\rho_{25} - \rho_{52}), \tag{2}$$

$$\dot{\rho}_{44} = -\Gamma_{42}\rho_{44} - \frac{i}{2}\Omega_c a_{42}(\rho_{24} - \rho_{42}), \tag{3}$$

$$\dot{\rho}_{33} = -\Gamma_{32}\rho_{33} - \frac{i}{2}\Omega_c a_{32}(\rho_{23} - \rho_{32}), \tag{4}$$

$$\begin{aligned}\dot{\rho}_{22} = {} & -\Gamma_{21}\rho_{22} + \Gamma_{32}\rho_{33} + \Gamma_{42}\rho_{44} + \Gamma_{52}\rho_{55} \\ & - \frac{i}{2}\Omega_p(\rho_{12} - \rho_{21}) - \frac{i}{2}\Omega_c a_{32}(\rho_{32} - \rho_{23}) \\ & - \frac{i}{2}\Omega_c a_{42}(\rho_{42} - \rho_{24}) - \frac{i}{2}\Omega_c a_{52}(\rho_{52} - \rho_{25}),\end{aligned} \tag{5}$$

$$\dot{\rho}_{11} = \Gamma_{21}\rho_{22} - \frac{i}{2}\Omega_p(\rho_{21} - \rho_{12}), \tag{6}$$

$$\dot{\rho}_{54} = [-i(\delta_1 + \delta_2) - \gamma_{54}]\rho_{54} + \frac{i}{2}\Omega_c a_{42}\rho_{52} - \frac{i}{2}\Omega_c a_{52}\rho_{24}, \tag{7}$$

$$\dot{\rho}_{53} = (-i\delta_2 - \gamma_{53})\rho_{53} + \frac{i}{2}\Omega_c a_{32}\rho_{52} - \frac{i}{2}\Omega_c a_{52}\rho_{23}, \tag{8}$$

$$\begin{aligned}\dot{\rho}_{52} = {} & [i(\Delta_c - \delta_2) - \gamma_{52}]\rho_{52} + \frac{i}{2}\Omega_p\rho_{51} + \frac{i}{2}\Omega_c a_{32}\rho_{53} \\ & + \frac{i}{2}\Omega_c a_{42}\rho_{54} + \frac{i}{2}\Omega_c a_{52}(\rho_{55} - \rho_{22}),\end{aligned} \tag{9}$$

$$\dot{\rho}_{51} = [i(\Delta_c + \Delta_p - \delta_2) - \gamma_{51}]\rho_{51} + \frac{i}{2}\Omega_p\rho_{52} - \frac{i}{2}\Omega_c a_{52}\rho_{21}, \tag{10}$$

$$\dot{\rho}_{43} = [-i\delta_1 - \gamma_{43}]\rho_{43} - \frac{i}{2}\Omega_c a_{42}\rho_{23} + \frac{i}{2}\Omega_c a_{32}\rho_{42}, \tag{11}$$

$$\begin{aligned}\dot{\rho}_{42} = {} & [i(\Delta_c + \delta_1) - \gamma_{42}]\rho_{42} + \frac{i}{2}\Omega_p\rho_{41} + \frac{i}{2}\Omega_c a_{32}\rho_{43} \\ & + \frac{i}{2}\Omega_c a_{52}\rho_{45} + \frac{i}{2}\Omega_c a_{42}(\rho_{44} - \rho_{22}),\end{aligned} \tag{12}$$

$$\dot{\rho}_{41} = [i(\Delta_c + \Delta_p + \delta_1) - \gamma_{41}]\rho_{41} + \frac{i}{2}\Omega_p\rho_{42} - \frac{i}{2}\Omega_c a_{42}\rho_{21}, \tag{13}$$

$$\dot{\rho}_{32} = (i\Delta_c - \gamma_{32})\rho_{32} + \frac{i}{2}\Omega_p\rho_{31} + \frac{i}{2}\Omega_c a_{32}(\rho_{33} - \rho_{22}) + \frac{i}{2}\Omega_c a_{42}\rho_{34} + \frac{i}{2}\Omega_c a_{52}\rho_{35}, \tag{14}$$

$$\dot{\rho}_{31} = [i(\Delta_c + \Delta_p) - \gamma_{31}]\rho_{31} + \frac{i}{2}\Omega_p\rho_{32} - \frac{i}{2}\Omega_c a_{32}\rho_{21}, \tag{15}$$

$$\dot{\rho}_{21} = (i\Delta_p - \gamma_{21})\rho_{21} + \frac{i}{2}\Omega_p(\rho_{22} - \rho_{11}) - \frac{i}{2}\Omega_c a_{32}\rho_{31}, - \frac{i}{2}\Omega_c a_{42}\rho_{41} - \frac{i}{2}\Omega_c a_{52}\rho_{51}, \tag{16}$$

$$\rho_{ki} = \rho_{ik}^*, \tag{17}$$

$$\rho_{11} + \rho_{22} + \rho_{33} + \rho_{44} + \rho_{55} = 1, \tag{18}$$

where i is the complex number; $\Omega_p = d_{21}E_p/\hbar$ and $\Omega_c = d_{32}E_c/\hbar$ are Rabi frequencies; d_{kl} is an element of dipole moment of the $|k\rangle - |l\rangle$ transition; $a_{32} = d_{32}/d_{32}$, $a_{42} = d_{42}/d_{32}$, and $a_{52} = d_{52}/d_{32}$ are the relative transition strengths; and γ_{kl} is the decay rate of the atomic coherence ρ_{kl}, given by [35]

$$\gamma_{kl} = \frac{1}{2}\left(\sum_{E_k<E_j}\Gamma_{jk} + \sum_{E_m<E_l}\Gamma_{lm}\right), \tag{19}$$

where Γ_{kl} is the decay rate of population from level $|k\rangle$ to level $|l\rangle$.

In a steady regime, the solution for the matrix element ρ_{21} can be calculated up to the third-order as [37]

$$\rho_{21} = \rho_{21}^{(1)} + \rho_{21}^{(3)} = -\frac{i\Omega_p}{2F} + \frac{i\Omega_p}{2F}\left[\frac{\Omega_p^2}{2\Gamma_{21}}\left(\frac{1}{F} + \frac{1}{F^*}\right)\right], \tag{20}$$

where

$$F = \gamma_{21} - i\Delta_p + \frac{a_{32}^2(\Omega_c/2)^2}{\gamma_{31} - i(\Delta_p + \Delta_c)} + \frac{a_{42}^2(\Omega_c/2)^2}{\gamma_{41} - i(\Delta_p + \Delta_c + \delta_1)}, + \frac{a_{52}^2(\Omega_c/2)^2}{\gamma_{51} - i(\Delta_p + \Delta_c - \delta_2)}, \tag{21}$$

and F^* is conjugation of F.

The total susceptibility can then be determined by the following relation:

$$\chi = -2\frac{Nd_{21}}{\varepsilon_0 E_p}\rho_{21}, \tag{22}$$

where N is the density of particles and ε_0 is the permittivity in vacuum.

In order to extract the first- and third-order susceptibilities, we interpret the total susceptibility in Eq. (22) in an alternative form:

$$\chi = \chi^{(1)} + 3E_p^2\chi^{(3)}. \tag{23}$$

Finally, the first-order and third-order susceptibilities are given as [37]

$$\chi^{(1)} = \frac{Nd_{21}^2}{\varepsilon_0\hbar}\left(\frac{A}{A^2 + B^2} + i\frac{B}{A^2 + B^2}\right), \tag{24}$$

$$\chi^{(3)} = -\frac{Nd_{21}^4}{3\varepsilon_0\hbar^3}\frac{1}{\Gamma_{21}}\frac{B}{A^2 + B^2}\left(\frac{A}{A^2 + B^2} + i\frac{B}{A^2 + B^2}\right), \tag{25}$$

where A and B are controllable parameters given by

$$A = -\Delta_p + \frac{A_{32}}{\gamma_{31}} + \frac{A_{42}}{\gamma_{41}} + \frac{A_{52}}{\gamma_{51}}, \tag{26}$$

$$B = \gamma_{21} + \frac{A_{32}}{\Delta_p + \Delta_c} + \frac{A_{42}}{\Delta_p + \Delta_c + \delta_1} + \frac{A_{52}}{\Delta_p + \Delta_c - \delta_2}, \tag{27}$$

$$A_{32} = \frac{\gamma_{31}(\Delta_p + \Delta_c)}{\gamma_{31}^2 + (\Delta_p + \Delta_c)^2}a_{32}^2(\Omega_c/2)^2, \tag{28}$$

$$A_{42} = \frac{\gamma_{41}(\Delta_p + \Delta_c + \delta_1)}{\gamma_{41}^2 + (\Delta_p + \Delta_c + \delta_1)^2}a_{42}^2(\Omega_c/2)^2, \tag{29}$$

$$A_{52} = \frac{\gamma_{51}(\Delta_p + \Delta_c - \delta_2)}{\gamma_{51}^2 + (\Delta_p + \Delta_c - \delta_2)^2}a_{52}^2(\Omega_c/2)^2. \tag{30}$$

From the linear and third-order susceptibilities, the linear index n_0 and self-Kerr nonlinear coefficient n_2 for the probe light are derived as

$$n_0 = 1 + \frac{\mathrm{Re}(\chi^{(1)})}{2} = 1 + \frac{Nd_{21}^2}{2\varepsilon_0\hbar}\frac{A}{A^2 + B^2}, \tag{31}$$

$$n_2 = \frac{3\mathrm{Re}(\chi^{(3)})}{4\varepsilon_0 n_0^2 c} = -\frac{Nd_{21}^4}{4\varepsilon_0^2\hbar^3 c}\frac{1}{\Gamma_{21}}\frac{AB}{\left(1 + \frac{Nd_{21}^2}{2\varepsilon_0\hbar}\frac{A}{A^2+B^2}\right)(A^2 + B^2)^2}. \tag{32}$$

In the case of absence of self-Kerr nonlinearity, the group index is determined by

$$n_g^{(0)} = n_0 + \omega_p\frac{\partial n_0}{\partial\omega_p} \simeq \omega_p\frac{Nd_{21}^2}{2\varepsilon_0\hbar}\left[\frac{A'(A^2 + B^2) - 2A(AA' + BB')}{(A^2 + B^2)^2}\right], \tag{33}$$

where A' and B' represent the derivatives of A and B over ω_p, respectively:

$$A' = -1 + \frac{A_{32}}{\gamma_{31}(\Delta_p + \Delta_c)} - \frac{2A_{32}^2}{a_{32}^2(\Omega_c/2)^2\gamma_{31}^2} + \frac{A_{42}}{\gamma_{41}(\Delta_p + \Delta_c + \delta_1)} - \frac{2A_{42}^2}{a_{42}^2(\Omega_c/2)^2\gamma_{41}^2} + \frac{A_{52}}{\gamma_{51}(\Delta_p + \Delta_c - \delta_2)} - \frac{2A_{52}^2}{a_{52}^2(\Omega_c/2)^2\gamma_{51}^2}, \tag{34}$$

$$B' = -\frac{2A_{32}^2}{a_{32}^2(\Omega_c/2)^2\gamma_{31}(\Delta_p + \Delta_c)} - \frac{2A_{42}^2}{a_{42}^2(\Omega_c/2)^2\gamma_{41}(\Delta_p + \Delta_c + \delta_1)} - \frac{2A_{52}^2}{a_{52}^2(\Omega_c/2)^2\gamma_{51}(\Delta_p + \Delta_c - \delta_2)}. \quad (35)$$

It is noted that there are three EIT windows centered at probe frequencies given by the two-photon resonance conditions: $\Delta_p + \Delta_c = 0$, $\Delta_p + \Delta_c + \delta_1 = 0$, and $\Delta_p + \Delta_c - \delta_2 = 0$ [35]. Therefore, the group index in each EIT window can be approximated by

$$n_g^{(0)}|_{32} \simeq \omega_p \frac{\partial n_0}{\partial \omega_p}\bigg|_{\Delta_p+\Delta_c=0} = \frac{2\omega_p N d_{21}^2}{\varepsilon_0 \hbar} \frac{a_{32}^2\Omega_c^2 - 4\gamma_{31}^2}{(a_{32}^2\Omega_c^2 + 4\gamma_{21}\gamma_{31})^2}, \quad (36)$$

$$n_g^{(0)}|_{42} \simeq \omega_p \frac{\partial n_0}{\partial \omega_p}\bigg|_{\Delta_p+\Delta_c+\delta_1=0} = \frac{2\omega_p N d_{21}^2}{\varepsilon_0 \hbar} \frac{(a_{42}^2\Omega_c^2 - 4\gamma_{41}^2)[(a_{42}^2\Omega_c^2 + 4\gamma_{21}\gamma_{41})^2 - (4\delta_1\gamma_{41})^2]}{[(4\delta_1\gamma_{41})^2 + (a_{42}^2\Omega_c^2 + 4\gamma_{21}\gamma_{41})^2]^2}, \quad (37)$$

$$n_g^{(0)}|_{52} \simeq \omega_p \frac{\partial n_0}{\partial \omega_p}\bigg|_{\Delta_p+\Delta_c-\delta_2=0}, = \frac{2\omega_p N d_{21}^2}{\varepsilon_0 \hbar} \frac{(a_{52}^2\Omega_c^2 - 4\gamma_{51}^2)[(a_{52}^2\Omega_c^2 + 4\gamma_{21}\gamma_{51})^2 - (4\delta_2\gamma_{51})^2]}{[(4\delta_2\gamma_{51})^2 + (a_{52}^2\Omega_c^2 + 4\gamma_{21}\gamma_{51})^2]^2}, \quad (38)$$

where $n_g^{(0)}|_{32}$, $n_g^{(0)}|_{42}$, and $n_g^{(0)}|_{52}$ are the group index at the EIT window in which the controlling field induces the transitions $|2\rangle \leftrightarrow |3\rangle$, $|2\rangle \leftrightarrow |4\rangle$, and $|2\rangle \leftrightarrow |5\rangle$, respectively.

In the presence of the self-Kerr nonlinearity, the effective index for the probe light (with intensity I_p) is determined by

$$n = n_0 + n_2 I_p. \quad (39)$$

The group index under presence of self-Kerr nonlinearity can therefore be determined as [43]

$$n_g^{(K)} = n + \omega_p \frac{\partial n}{\partial \omega_p} = n_0 + n_2 I_p + \omega_p \left(\frac{\partial n_0}{\partial \omega_p} + \frac{\partial n_2}{\partial \omega_p} I_p \right), \quad (40)$$

where n_0 and n_2 are the linear and nonlinear refractive indices determined by Eqs. (31) and (32), respectively.

3. APPLICATION TO ^{85}Rb ATOMIC MEDIUM

In order to illustrate applications of the analytic model, we apply to a cold atomic medium of ^{85}Rb, where the Doppler effect can be ignored. The states, $|1\rangle$, $|2\rangle$, $|3\rangle$, $|4\rangle$, and $|5\rangle$, are chosen as $5S_{1/2}(F = 3)$, $5P_{3/2}(F' = 3)$, $5D_{5/2}(F'' = 3)$, $5D_{5/2}(F'' = 4)$, and $5D_{5/2}(F'' = 2)$, respectively. The atomic parameters are given [35,44]: $N = 5 \times 10^{11}$ atoms/cm^3; $\Gamma_{32} = \Gamma_{42} = \Gamma_{52} = 2\pi \times 0.97$ MHz; $\Gamma_{21} = 2\pi \times 6$ MHz; $\delta_1 = 2\pi \times 9$ MHz; $\delta_2 = 2\pi \times 7.6$ MHz; $d_{21} = 1.6 \times 10^{-29}$ C · m; $\omega_p = 2\pi \times 3.77 \times 10^8$ MHz; and $a_{32}:a_{42}:a_{52} = 1:1.4:0.6$.

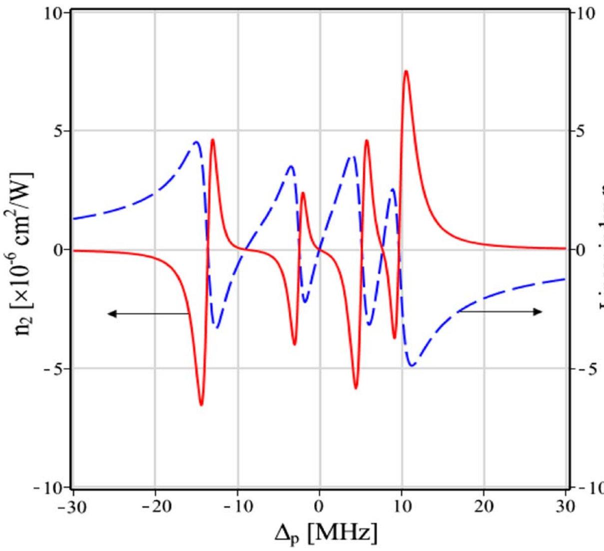

Fig. 2. Variations of the self-Kerr nonlinearity n_2 (solid) and linear index of refraction n_0 (dashed) versus the probe frequency detuning Δ_p when $\Omega_c = 10$ MHz and $\Delta_c = 0$.

In order to see variations of linear and nonlinear indices, we plotted the linear index n_0 and Kerr nonlinearity n_2 versus the probe frequency detuning Δ_p for the fixed parameters $\Omega_c = 10$ MHz and $\Delta_c = 0$, as in Fig. 2. From Fig. 2, we can see a normal and anomalous dispersion of the linear index (dashed curve) in three separated regions corresponding to three EIT windows that center at $\Delta_p = -9$ MHz, $\Delta_p = 0$, and $\Delta_p = 7.6$ MHz [35]. Such a dispersive property delivers both sub- and superluminal propagation modes for the multi-frequency probe light. On the other hand, the dispersion of the linear index is in the opposite direction from that of the self-Kerr nonlinearity (solid curve in Fig. 2); thus, the giant self-Kerr nonlinearity can reduce the effective index or enhance the group velocity of the probe light [see Fig. 3(a)]. Furthermore, the self-Kerr nonlinearity leads to variation of both magnitude and sign of the group index under changing probe intensity; consequently, one may manipulate the probe light to propagate between sub- and superluminal mode by tuning its own intensity [Fig. 3(b)]. This variation can be explained from Eq. (40) in that the group index depends proportionally on intensity of the probe light; thus, the self-Kerr nonlinearity is more efficient with high intensity of the probe light.

In Fig. 4, we consider influence of the coupling field on the group index by plotting the $n_g^{(K)}$ versus the frequency detuning Δ_c (a) and the Rabi frequency Ω_c (b) for three EIT windows centered at $\Delta_p = -2$, $\Delta_p = -10$ MHz, and $\Delta_p = 8$ MHz. It is shown that the group index varies between negative and positive values with changing intensity and/or frequency of the coupling field. In other words, one may manipulate the probe light to propagate between sub- and superluminal mode by controlling and/or frequency of the coupling field. This can be explained by noticing that magnitude and sign of both linear and nonlinear indices depend sensitively on intensity and/or

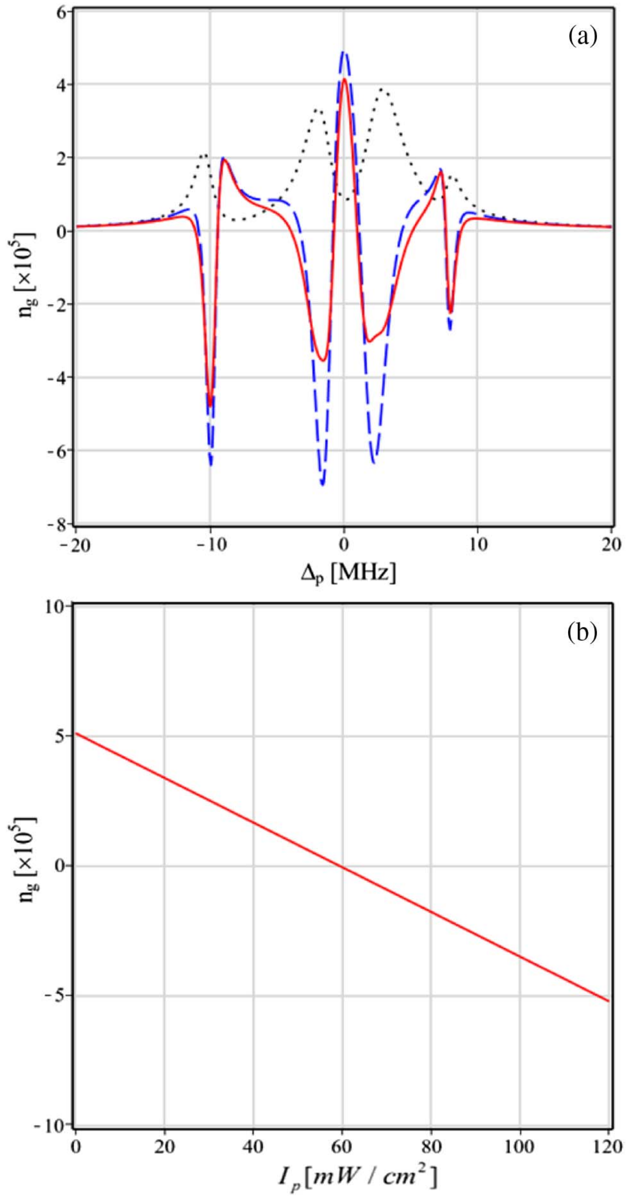

Fig. 3. (a) Variation of the group index versus probe frequency detuning in the case of self-Kerr nonlinearity absent (dashed) and present (solid) when $I_p = 10\ \mathrm{mW/cm^2}$, $\Omega_c = 4$ MHz, and $\Delta_c = 0$; the dotted curve represents EIT spectrum plotted from the imaginary part of Eq. (24). (b) Variation of the Kerr nonlinearity $n_g^{(K)}$ versus probe intensity I_p when $\Omega_c = 4$ MHz and $\Delta_c = \Delta_p = 0$.

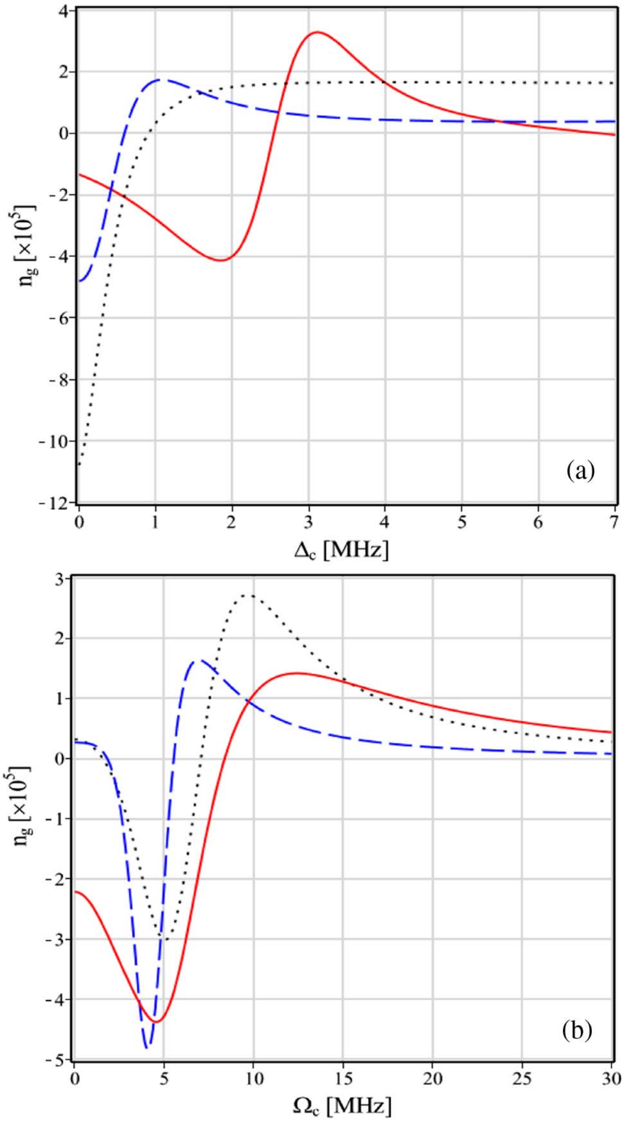

Fig. 4. Variations of $n_g^{(K)}$ versus Δ_c when $\Omega_c = 4$ MHz (a) and versus Ω_c when $\Delta_c = 0$ (b) at $I_p = 10\ \mathrm{mW/cm^2}$ and $\Delta_p = -2$ MHz (solid), $\Delta_p = -10$ MHz (dashed), and $\Delta_p = 8$ MHz (dotted).

frequency of the coupling field [35,37]. On the other hand, it should be noted from Fig. 4(a) that variation of coupling frequency while keeping probe frequency may cause significant absorption outside the EIT widows [35].

4. DISCUSSION

In principle, the five-level cascade-type scheme can be used for any atomic or molecular system having the energy structure as in Fig. 1. At first, we showed an advantage of the analytic model for estimating an achievable minimum group velocity of the probe light. Indeed, based on Eq. (36), the group index (or the group velocity) is maximized (or minimized) at the following Rabi frequency:

$$\Omega_c = 2\sqrt{(\gamma_{21} + 2\gamma_{31})\gamma_{31}}. \tag{41}$$

At such Rabi frequency, the minimum group velocity in the first EIT window is determined as

$$(v_{g32}^{(0)})_{\min} = \frac{8\varepsilon_0 \hbar c}{\omega_p N d_{21}^2}(\gamma_{21} + \gamma_{31})\gamma_{31}. \tag{42}$$

It is shown from Eq. (42) that the group velocity depends on the damping rate γ_{31} or depends inversely on lifetimes of the excited electronic states. For the excited states having lifetimes of a few ns, the minimum group velocity can be a few m/s, as shown in Ref. [6]. However, the cascade excitation scheme delivers a possible way to choose the uppermost excited states as the Rydberg states, which have lifetimes of a few μs (lifetime of the state $38D_{5/2}$ of Rb atom is 13 μs, see Ref. [45], e.g.). In this case, one may slow down the probe light to a few mm/s (ultraslow light). On the other hand, from Eq. (42), one may further slow down group velocity of the probe light by increasing the atomic density.

From a practical aspect, it is worth to evaluate the value of transparency efficiency at which the group index maximizes. For the EIT window at $\Delta_p = 0$, the transparency efficiency is given as [35]

$$R_{32} = \frac{\alpha(0) - \alpha(\Omega_c)}{\alpha(0)} = \frac{a_{32}^2\Omega_c^2}{4\gamma_{21}\gamma_{31} + a_{32}^2\Omega_c^2}, \quad (43)$$

where $\alpha(0)$ and $\alpha(\Omega_c)$ are the absorption coefficient when the controlling laser turns off and on. Substituting Eq. (41) into Eq. (43), we have

$$R_{32} = \frac{1}{2}\left(1 + \frac{\gamma_{31}}{\gamma_{21} + \gamma_{31}}\right). \quad (44)$$

On the other hand, from Eqs. (36) and (43), we found an expression of the group index as a function of the transparency efficiency as follows:

$$n_{g32}^{(0)} = \frac{2\omega_p N d_{21}^2}{\varepsilon_0 \hbar}\left[\frac{R_{32}(1 - R_{32})}{4\gamma_{21}\gamma_{31}} - \frac{(1 - R_{32})^2}{4\gamma_{21}^2}\right]. \quad (45)$$

Variation of the group index versus the transparency depth is plotted in Fig. 5. One can clearly see that the maximum group index occurs at the transparency efficiency equal to approximately 60% (for ^{85}Rb atoms), which agrees with Eq. (44).

Finally, we compared the theoretical result with a prominent observation in Ref. [6] by restricting the coupling parameters $A_{52} = A_{42} = 0$ in Eqs. (33) and (40) to reduce the five- to three-level excitation scheme. The group velocity is plotted versus the coupling Rabi frequency under the presence (solid) and absence (dashed) of the self-Kerr nonlinearity, where all parameters are given as the same as in Ref. [6], as shown in Fig. 6. It should be noted that the measured value of group velocity $v_g = 17$ m/s is attained at $I_c = 12$ mW/cm^2 (corresponding $\Omega_c = 5.3$ MHz), whereas the theoretical value at the same parameters is $v_g = 17$ m/s or $v_g = 15$ m/s for the presence or absence of the self-Kerr nonlinearity, respectively. This comparison shows that the model is more accurate with the inclusion of the self-Kerr nonlinearity. Indeed, whenever the self-Kerr nonlinearity is excluded, deviation will be greater at higher probe intensity, which is 10% at $I_p = 5$ mW/cm^2. On the other hand, Fig. 6 shows a possible optimization to further slow down the probe light by reducing its own intensity to an ideal case (without influence of the self-Kerr nonlinearity).

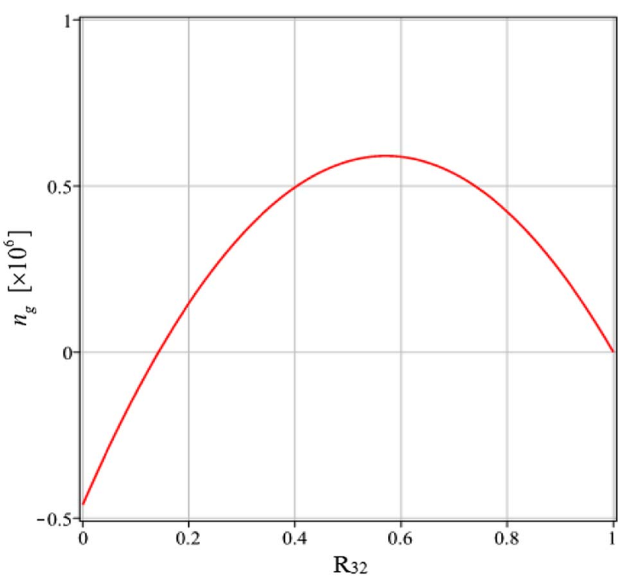

Fig. 5. Variation of group index $n_{g32}^{(0)}$ versus the transparency efficiency R_{32} at $\Delta_p = \Delta_c = 0$.

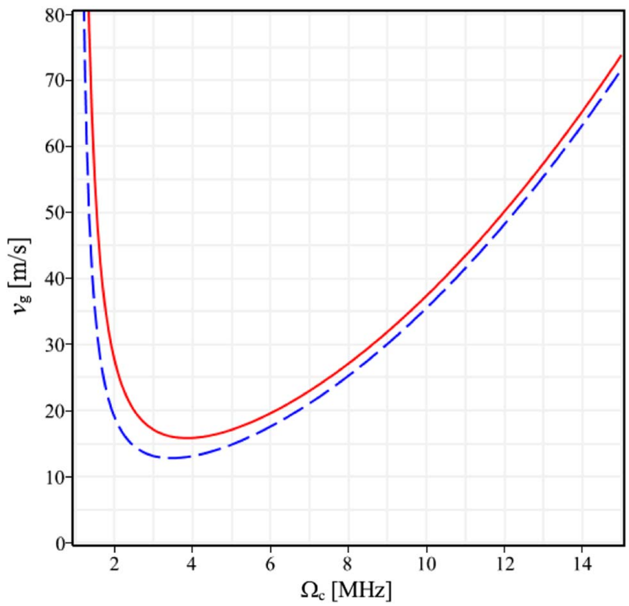

Fig. 6. Plot of the group velocity versus the Rabi frequency Ω_c of the coupling field under the presence (solid) and absence (dashed) of the self-Kerr nonlinearity when $I_p = 5$ mW/cm^2, and $\Delta_p = \Delta_c = 0$.

5. CONCLUSION

We have proposed a model for manipulation of a multi-frequency probe light in a five-level cascade-type medium in the presence of the self-Kerr nonlinearity. The group index for the probe light is derived as an analytic function of the parameters of the light fields, atomic density, and atomic electronic lifetimes. Although the self-Kerr nonlinearity enhances group velocity, one may use the probe and/or coupling fields as knobs to manipulate the probe light between the subluminal and superluminal modes in three separated frequency regions. The model agrees with experimental observation, and it is helpful in finding the optimized parameters and related applications. Based on the cascade excitation scheme, it could be possible to choose the uppermost excited electronic states having long lifetimes, as Rydberg states, to manipulate group velocity of light to a few mm/s.

Funding. Vietnam Ministry of Science and Technology (ĐTĐLCN.17/17).

REFERENCES

1. M. Fleischhauer and M. D. Lukin, “Dark-state polaritons in electromagnetically induced transparency,” Phys. Rev. Lett. **84**, 5094–5097 (2000).
2. M. D. Lukin, “Colloquium: trapping and manipulating photon states in atomic ensembles,” Rev. Mod. Phys. **75**, 457–472 (2003).
3. R. W. Boyd and D. J. Gauthier, “Controlling the velocity of light pulses,” Science **326**, 1074–1077 (2009).
4. R. W. Boyd, “Slow and fast light: fundamentals and applications,” J. Mod. Opt. **56**, 1908–1915 (2009).
5. M. Fleischhauer, I. Mamoglu, and J. P. Marangos, “Electromagnetically induced transparency: optics in coherent media,” Rev. Mod. Phys. **77**, 633–673 (2005).
6. L. V. Hau, S. E. Harris, Z. Dutton, and C. H. Bejroozi, “Light speed reduction to 17 metres per second in an ultracold atomic gas,” Nature **397**, 594–598 (1999).
7. M. M. Kash, V. A. Sautenkov, A. S. Zibrov, L. Hollberg, G. R. Welch, M. D. Lukin, Y. Rostovtsev, E. S. Fry, and M. O. Scully, “Ultraslow group velocity and enhanced nonlinear optical effects in a coherently driven hot atomic gas,” Phys. Rev. Lett. **82**, 5229–5232 (1999).
8. D. Budker, D. F. Kimball, S. M. Rochester, and V. V. Yashchuk, “Nonlinear magneto-optics and reduced group velocity of light in atomic vapor with slow ground state relaxation,” Phys. Rev. Lett. **83**, 1767–1770 (1999).
9. A. V. Turukhin, V. S. Sudarshanam, M. S. Shahriar, J. A. Musser, B. S. Ham, and P. R. Hammer, “Observation of ultraslow and stored light pulses in a solid,” Phys. Rev. Lett. **88**, 023602 (2002).
10. K. Bencheikh, E. Baldit, S. Briaudeau, P. Monnier, J. A. Levenson, and G. Mélin, “Slow light propagation in a ring erbium-doped fiber,” Opt. Express **18**, 25642–25648 (2010).
11. L. J. Wang, A. Kuzmich, and A. Dogariu, “Gain-assisted superluminal light propagation,” Nature **406**, 277–279 (2000).
12. E. E. Mikhailov, V. A. Sautenkov, I. Novikova, and G. R. Welch, “Large negative and positive delay of optical pulses in coherently prepared dense Rb vapor with buffer gas,” Phys. Rev. A **69**, 063808 (2004).
13. E. E. Mikhailov, V. A. Sautenkov, Y. V. Rostovtsev, and G. R. Welch, “Absorption resonance and large negative delay in rubidium vapor with a buffer gas,” J. Opt. Soc. Am. B **21**, 425–428 (2004).
14. A. M. Akulshin and R. J. McLean, “Fast light in atomic media,” J. Opt. **12**, 104001 (2010).
15. G. S. Agarwal, T. N. Dey, and S. Menon, “Knob for changing light propagation from subluminal to superluminal,” Phys. Rev. A **64**, 053809 (2001).
16. K. Kim, H. S. Moon, C. Lee, S. K. Kim, and J. B. Kim, “Observation of arbitrary group velocities of light from superluminal to subluminal on a single atomic transition line,” Phys. Rev. A **68**, 013810 (2003).
17. H. Sun, H. Guo, Y. Bai, D. Han, S. Fan, and X. Chen, “Light propagation from subluminal to superluminal in a three-level Λ-type system,” Phys. Lett. A **335**, 68–75 (2005).
18. M. Mahmoudi, M. Sahrai, and H. Tajalli, “Subluminal and superluminal light propagation via interference of incoherent pump fields,” Phys. Lett. A **357** 66–71 (2006).
19. D. Han, Y. Zeng, Y. Bai, H. Cao, W. Chen, C. Huang, and H. Lu, “Controlling the group velocity in a five-level K-type atomic system,” Opt. Commun. **281**, 4712–4714 (2008).
20. I. H. Bae and H. S. Moon, “Continuous control of light group velocity from subluminal to superluminal propagation with a standing-wave coupling field in a Rb vapor cell,” Phys. Rev. A **83**, 053806 (2011).
21. K. Qian, L. Zhan, L. Zhang, Z. Q. Zhu, J. S. Peng, Z. C. Gu, X. Hu, S. Y. Luo, and Y. X. Xia, “Group velocity manipulation in active fibers using mutually modulated cross-gain modulation: from ultraslow to superluminal propagation,” Opt. Lett. **36**, 2185–2187 (2011).
22. S. Dutta, “The incoherent pump rate: an optical tool for controlling the probe response and dispersion in a three-level Λ system in the presence of spontaneously generated coherence,” Phys. Scr. **83**, 015401 (2011).
23. V. Bharti and V. Natarajan, “Sub- and super-luminal light propagation using a Rydberg state,” Opt. Commun. **392**, 180–184 (2017).
24. M. J. Akram, M. M. Khan, and F. Saif, “Tunable fast and slow light in a hybrid optomechanical system,” Phys. Rev. A **92**, 023846 (2015).
25. Q. Jang, Y. Zhang, D. Wang, S. Ahrens, J. Zhang, and S. Zhu, “Superluminal reflection and transmission of light pulses via resonant four-wave mixing in cesium vapor,” Opt. Express **24**, 24451–24459 (2016).
26. H. Schmidt and A. Imamogdlu, “Giant Kerr nonlinearities obtained by electromagnetically induced transparency,” Opt. Lett. **21**, 1936–1938 (1996).
27. H. Wang, D. Goorskey, and M. Xiao, “Enhanced Kerr nonlinearity via atomic coherence in a three-level atomic system,” Phys. Rev. Lett. **87**, 073601 (2001).
28. T. N. Dey and G. S. Agarwal, “Observable effects of Kerr nonlinearity on slow light,” Phys. Rev. A **76**, 015802 (2007).
29. H. Ali, Ziauddin, and I. Ahmad, “The effect of Kerr nonlinearity and Doppler broadening on slow light propagation,” Laser Phys. **24**, 025201 (2014).
30. D. Mc Gloin, D. J. Fullton, and M. H. Dunn, “Electromagnetically induced transparency in N-level cascade schemes,” Opt. Commun. **190**, 221–229 (2001).
31. E. Paspalakis and P. L. Knight, “Electromagnetically induced transparency and controlled group velocity in a multilevel system,” Phys. Rev. A **66**, 015802 (2002).
32. K. Yadav and A. Wasan, “Sub-luminal and super-luminal light propagation in inverted-Y system with wavelength mismatching effects,” Phys. Lett. A **381**, 3246–3253 (2017).
33. J. Wang, L. B. Kong, X. H. Tu, K. J. Jiang, K. Li, H. W. Xiong, Y. Zhu, and M. S. Zhan, “Electromagnetically induced transparency in multi-level cascade scheme of cold rubidium atoms,” Phys. Lett. A **328**, 437–443 (2004).
34. M. D. Lukin and A. Imamoglu, “Nonlinear optics and quantum entanglement of ultraslow single photons,” Phys. Rev. Lett. **84**, 1419–1422 (2000).
35. L. V. Doai, P. V. Trong, D. X. Khoa, and N. H. Bang, “Electromagnetically induced transparency in five-level cascade scheme of ^{85}Rb atoms: an analytical approach,” Optik **125**, 3666–3669 (2014).
36. D. X. Khoa, P. V. Trong, L. V. Doai, and N. H. Bang, “Electromagnetically induced transparency in a five-level cascade system under Doppler broadening: an analytical approach,” Phys. Scr. **91**, 035401 (2016).
37. D. X. Khoa, L. V. Doai, D. H. Son, and N. H. Bang, “Enhancement of self-Kerr nonlinearity via electromagnetically induced transparency in a five-level cascade system: an analytical approach,” J. Opt. Soc. Am. B **31**, 1330–1334 (2014).
38. L. V. Doai, D. X. Khoa, and N. H. Bang, “EIT enhanced self-Kerr nonlinearity in the three-level lambda system under Doppler broadening,” Phys. Scr. **90**, 045502 (2015).
39. D. X. Khoa, L. V. Doai, L. N. M. Anh, L. C. Trung, P. V. Thuan, N. T. Dung, and N. H. Bang, “Optical bistability in a five-level cascade EIT medium: an analytical approach,” J. Opt. Soc. Am. B **33**, 735–740 (2016).
40. R. Kumar, V. Gokhroo, and S. N. Chormaic, “Multi-level cascaded electromagnetically induced transparency in cold atoms using an optical nanofibre interface,” New J. Phys. **17**, 123012 (2015).
41. D. X. Khoa, H. M. Dong, L. V. Doai, and N. H. Bang, “Propagation of laser pulse in a three-level cascade inhomogeneously broadened medium under electromagnetically induced transparency conditions,” Optik **131**, 497–505 (2017).
42. D. X. Khoa, L. C. Trung, P. V. Thuan, L. V. Doai, and N. H. Bang, “Measurement of dispersive profile of a multi-window EIT spectrum in a Doppler-broadened atomic medium,” J. Opt. Soc. Am. B **34**, 1255–1263 (2017).
43. H. Wu and M. Xiao, “Cavity linewidth narrowing and broadening due to competing linear and nonlinear dispersions,” Opt. Lett. **32**, 3122–3124 (2007).
44. D. A. Steck, “^{85}Rb D Line Data,” http://steck.us/alkalidata.
45. M. Mack, J. Grimmel, F. Karlewski, L. Sárkány, H. Hattermann, and J. Fortágh, “All-optical measurement of Rydberg-state lifetimes,” Phys. Rev. A **92**, 012517 (2015).